Available online at www.sciencedirect.com

ScienceDirect

Energy Procedia 137 (2017) 204–213

Energy Procedia

www.elsevier.com/locate/procedia

14th Deep Sea Offshore Wind R&D Conference, EERA DeepWind'2017, 18-20 January 2017, Trondheim, Norway

Diagnostic monitoring of drivetrain in a 5 MW spar-type floating wind turbine using Hilbert spectral analysis

Mahdi Ghane[a,b,*], Amir R.Nejad[a], Mogens Blanke[b,c], Zhen Gao[a,b], Torgeir Moan[a,b]

[a] *Department of Marine Technology, NTNU, Trondheim, Norway*

[b] *Center for Autonomous Marine Operations and Systems, NTNU, Trondheim, Norway*

[c] *Department of Electrical Engineering, Technical University of Denmark (DTU), DK 2800Kgs. Lyngby, Denmark*

Abstract

The objective of this paper is to investigate the frequency-based fault detection of a 5MW spar-type floating wind turbine (WT) gearbox using measurements of the global responses. It is extremely costly to seed managed defects in a real WT gearbox to investigate different fault detection and condition monitoring approaches; using analytical tools, therefore, is one of the promising approaches in this regard. In this study, forces and moments on the main shaft are obtained from the global response analysis using an aero-hydro-servo-elastic code, SIMO-RIFLEX-AeroDyn. Then, they are utilized as inputs to a high-fidelity gearbox model developed using a multi-body simulation software (SIMPACK). The main shaft bearing is one of the critical components since it protects gearbox from axial and radial loads. Six different fault cases with different severity in this bearing are investigated using power spectral density (PSD) of relative axial acceleration of the bearing and nacelle. It is shown that in severe degradation of this bearing the first stage dynamic of the gearbox is dominant in the main shaft vibration signal. Inside the gearbox, the bearings on the high speed side are those often with high probability of failure, thus, one fault case in IMS-B bearing was also considered. Based on the earlier studies, the angular velocity error function is considered as residual for this fault. The Hilbert transform is used to determine the envelope of this residual. Information on the amplitude of this residual properly indicates damage in this bearing.

Peer-review under responsibility of SINTEF Energi AS.

Keywords: Floating Wind Turbine; Wind Turbine Gearbox; Fault Detection; Envelope Analysis; Hilbert Transform; Condition Monitoring

1. Introduction

One of the main objectives in wind turbines (WT), like any power generation approach, is to lower the cost of energy (COE), which is the ratio between the total lifetime cost and the total generated energy during a WT lifetime. Unlike conventional power plants, wind turbines (WTs) are exposed to severe and highly variable environmental disturbances and, for floating turbines, also the fluctuating mechanical loads due to waves. These external factors

1876-6102 © 2017 The Authors. Published by Elsevier Ltd.
Peer-review under responsibility of SINTEF Energi AS.
10.1016/j.egypro.2017.10.374

contribute to large amount of downtime and high operation and maintenance (OM) costs during WTs typical operational lifetime of 20 years [1]. OM costs are estimated to be 10-15% of a total turbine cost for onshore WTs. Increase in WTs size and more WTs deployed offshore raises OM costs up to 20-25% of a total turbine cost for offshore WTs [2]. OM costs, therefore, represent a significant share of the total cost for offshore wind energy [2]. In this respect, condition monitoring (CM) can play a significant role.

Using condition-based maintenance (predictive maintenance) instead of periodic maintenance (preventive maintenance) maximize the reliability and minimize the maintenance cost of WTs [3]. Despite of the general development in WT industry, its condition monitoring is still premature. The use of other industries condition monitoring techniques needs adaption in order to be used in WT industry [3]. A failure mode, effects and criticality analysis (FMECA) is required to consider all the major assemblies and the effects of their failure on the overall turbine performance [4]. Many researchers have investigated the WT dynamic global responses due to different dominant failures [5, 6]. WTs undergo the highest downtime due to failure in gearboxes [7]; accordingly, effective signal processing for gearbox defect detection and diagnosis is becoming an active research area.

A review of wind turbine gearbox monitoring techniques using data acquisition and CM techniques was presented in [8]. CM techniques are classified into model-based and signal-based approaches with the common feature that residuals are generated to monitor changes in the system. Residuals are signals that are sensitive to faults but robust to noise and unknown disturbances [9, 10]. Model-based techniques may have high complexity and the modelling part may be a significant engineering effort [11, 12]. Reduced order model techniques are new approaches in the area to derive a wind turbine model for this purpose [13, 14]. On the other hand, signal-based approaches avoid dynamic modelling and look instead at changes in the properties of residual signal. Signal-based approaches include vibration-based, oil and debris analysis [15, 16] and non-destructive test, such as thermography and ultrasound analysis [17, 18]. Most of the WT gearbox failures initiate from bearing degradation [19, 20], as bearings protect gears from non-torque loads in axial and radial directions. Likelihood ratio test (a time-domain approach) was investigated in [21] to detect the fault in the main shaft bearing of a floating WT. Probabilistic neural network (PNN) and a simplified fuzzy adaptive resonance theory map (SFAM) were used in [22] to distinguish between seven bearing status. In many industrial applications, it is hard to access bearings inside a gearbox due to the location of the equipment and the choice of the implemented sensors; C.P. Mbo'o and K. Hameyer offered a bearing fault detection using the frequency analysis of stator current using linear discriminant analysis and the Bayes classifier [23].

In this study, the possibility of fault detection of damage in two different bearings in 5MW gearbox is investigated exploiting relative axial acceleration and angular velocity error function. The damage in this context is the worn condition - primarily due to fatigue - and initiation of fatigue cracks. Fatigue for rolling bearings is defined by ISO 15243 as "the change in the structure, which is caused by the repeated stress developed in the contacts between the rolling elements and the raceways" [24]. Such damage and degradation mechanism can be modelled by local stiffness reduction [25-27] which is employed in this paper.

The remainder of the paper is organized as follows. Section 2 gives a detailed explanation of the WT and the drivetrain model. Section 3 explains the seeded faults in SIMPACK and the detection methodology. Section 4 presents the fault detection results. Finally, Section 5 concludes the paper.

2. Wind turbine and drivetrain model

A 5 MW reference gearbox [28] mounted on the floating OC3 Hywind spar structure [29, 30] is used in this study. This WT is a 3-bladed upwind WT with characteristic features shown in Table 1. The spar-floating structure is a column-shaped structure connected by mooring lines to the seabed. The spar structures have a large draft and a small waterline area. The details of the spar structure analyzed in this paper were described by Nejad et al. [31]. The 5 MW reference gearbox used in this study was developed by Nejad et al. [28] for offshore WTs. The gearbox consists of three stages: two planetary and one parallel stage gears. Table 2 shows the general specifications of this gearbox. Fig.1

shows the gearbox and the drivetrain layout. The gearbox was designed with a 4-point support with two main bearings to reduce non-torque loads entering the gearbox.

Table 1: Wind turbine specifications [29, 30].

Parameter	Value
Type	Upwind/3 blades
Cut-in, rated and cut-out wind speed (m/s)	3, 11.4, 25
Hub height (m)	87.6
Rotor diameter (m)	126
Hub diameter (m)	3
Rotor mass (1,000 kg)	110
Nacelle mass (1,000 kg)	240
Hub mass (1,000 kg)	56.8

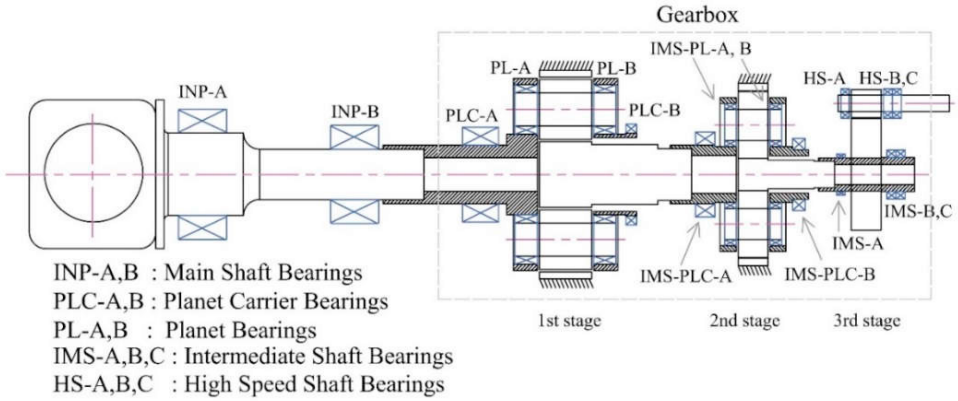

Figure 1: 5 MW reference gearbox layout [30].

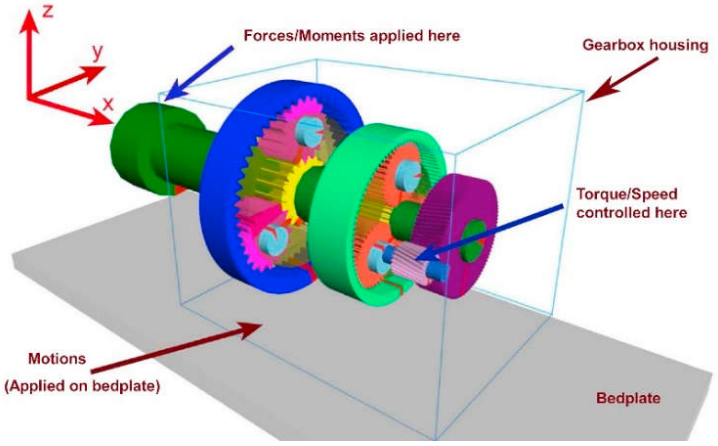

Figure 2: MBS model of the 5 MW reference gearbox [30]

The multi-body simulation (MBS) model of this gearbox is presented in Fig.2. As shown in the figure, the motions are applied on the bedplate and the external loads on the main shaft. The generator torque and speed is then controlled on the generator side [28]. The gearbox specification and critical frequencies of the gearbox are listed in Tables 2 and 3, respectively.

Table 2: 5 MW reference gearbox specification [28].

Parameter	Value
Type	2 Planetary + 1 Parallel
1st stage ratio	01:03.9
2nd stage ratio	01:06.2
3rd stage ratio	01:04.0
Total ratio	02:36.4
Designed power (kW)	5000
Rated input shaft speed (rpm)	12.1
Rated generator shaft speed (rpm)	1165.9
Rated input shaft torque (kN.m)	3946
Rated generator shaft torque (kN.m)	40.953
Total dry mass (1000 kg)	53
Service life (year)	20

Table 3: Critical frequencies in different stage of 5MW gearbox

Stage	Mesh freq. (Hz)
1st stage – carrier	11
1st stage – sun gear	14.8
2nd stage – carrier	73
2nd stage – planet	44

3. Methodology

3.1. De-coupled Approach & Environmental Condition

The decoupled analysis approach was employed in this study. First, the forces and moments on the main shaft were obtained from the global response analysis. Second, they were used as inputs to a detailed gearbox model, an MBS model, in which simulations with a higher-fidelity model and smaller time steps were performed. The global analysis was conducted using an aero-hydro-servo-elastic code, SIMO-RIFLEX-AeroDyn [32]. Simulations were carried out at the rated wind speed with wave conditions characterized by a significant wave height H_S = 5 m and a peak period T_P = 12 s (modeled by a JONSWAP spectrum). The turbulence intensity factor was taken to be 0.15 according to IEC 61400-1 [33]. The environmental data used in this study were obtained from a buoy off the coast of Portugal [34]. To minimize statistical uncertainties, six 3,800 s simulations were performed for each wind speed. The choice of one-hour simulations is a compromise between 10 minutes (typically in the wind industry) and 3 hours (offshore), and has been shown to be reasonable [35]. The first 200 s of data were removed during post-processing to eliminate the transient effects associated with start-up. In the MBS analysis, the bearings were modeled as force elements and obey force-deflection relations. The gears were modeled with compliance at the tooth and incorporate detailed tooth properties [28]. Earlier works on WT gearboxes based on the decoupled method include those by Xing et al. [36] and Nejad et al. [37, 38].

3.2. Fault Cases

Earlier studies [19, 22] have shown that the main bearings play an important role in reducing the non-torque loads entering the gearbox. Similarly, in a 4-point support drivetrain, the second main bearing, a spherical roller bearing, is the one that prevents the axial load entering the gearbox. Seven fault cases, representing different wear severity, were considered for the main shaft bearing. To have a better understanding of each fault cases in the main shaft bearing, ISO 20816-1 [39] is used to classify the fault cases based on the vibration level for different wear severity in INB-P bearing, Table.4. ISO 10816-21 introduced some vibration levels for horizontal axis wind turbines with gearbox; however, the given zone boundary values apply only to onshore wind turbine with nominal output of 3 MW or less. Hence, ISO 20816-1 is adopted here. This standard classifies four vibration zone boundaries, using the r.m.s of the velocity:
Zone A: new machines
Zone B: acceptable zone for long-term operation
Zone C: unacceptable for long-term operation
Zone D: can cause severe damage

INP-B bearing stiffness for different fault cases (K_{xf}) and relative value with respect to no-wear case (FC0, K_{xnf}) are also shown in Table. 4.

Table 4: Velocity r.m.s of the INP-B in different fault cases

Fault cases	K_{xf} (N/m)	$\frac{K_{xf}}{K_{xnf}} \times 100\%$	r.m.s (mm/s)	vibration zone boundary
FC0	4.06×10^8	100	0.8	A/B
FC1	3.86×10^8	95	0.9	A/B
FC2	3.45×10^8	85	0.9	A/B
FC3	2.84×10^8	70	2.2	B/C
FC4	2.03×10^8	50	2.4	B/C
FC5	1.22×10^8	30	8.3	C/D
FC6	4.06×10^7	10	7.7	C/D

For the bearings inside the gearbox, the IMS-B bearing, in higher speed stage was selected based on the vulnerability map developed by Nejad et al. [19]. We have tried– in another study and with another method [40]- to detect the fault in this bearing at 30% and lower damage but the results were not promising. Hence, we took this level as a testing point for the method described in this paper to identify this fault level for IMS-B bearing. The damage in the main bearing is in the axial direction while for the bearing inside the gearbox, it is in the radial direction.

3.3. Envelope analysis using the Hilbert transformation

Unlike the Fourier and Laplace transform, Hilbert transform does not involve a change of domain. The Hilbert transform of a signal in time (frequency) is another signal in time (frequency). The Hilbert transform of a real value time-domain signal, x(t), is defined by [41]:

$$H[\mathrm{x(t)}] = \frac{1}{\pi} \ \text{p.v.} \int_{-\infty}^{\infty} \frac{x(\tau)}{t-\tau} \, d\tau \tag{1}$$

where p.v. represents the Cauchy principle value. Equation (1) is the convolution of $x(t)$ and $(t) = 1/\pi t$, indicating a 90° phase shift in frequency domain; accordingly, the non-stationary characteristics of the modulating signal are not affected. The Hilbert transform, $H[\mathrm{x(t)}]$, is a complex time series, where the magnitude of this complex signal represents the envelope of the signal, an estimate of the amplitude modulation [42]. Vibration signals in many

rotating machineries have the same feature, i.e. a high frequency carrier and a low frequency signal bearing the information about faults in the system. Consequently, the Hilbert transform provides a practical tool to detect faults in bearings and gearboxes [43-45].

4. Results and Discussions

The choice of a residual, acceleration, velocity or displacement measurements, depends on the high relative amplitude of the residual and absence of disturbances in operating frequency range. One of the main advantages of accelerometers is the extremely wide range of both amplitude and frequency that they provide [46]. Relative axial acceleration of the main shaft and nacelle is the measurement which is less sensitive to components in wind and wave frequency range, Figs 3 and 4; accordingly, it is considered as the residual to detect wear in the main shaft bearing.

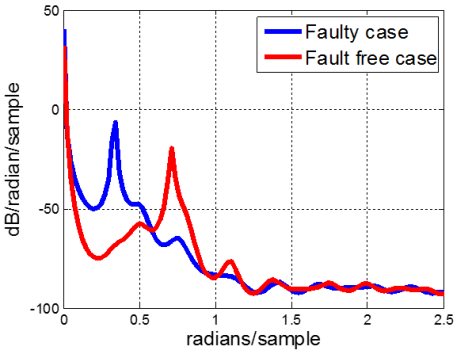

Figure 3: PSD of the main shaft axial acceleration.

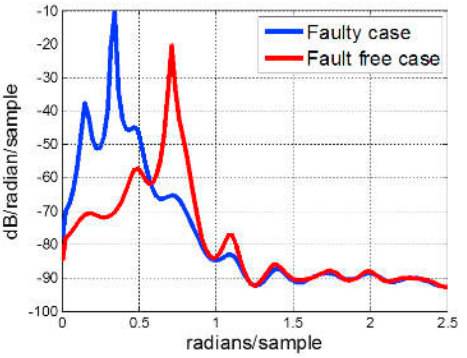

Figure 4: PSD of the relative acceleration of the main shaft and nacelle

The development of wear in bearings may be considered having very slow time constants, and is significant slower than the dynamics of the bearing itself; accordingly, it is practically possible to perform windowed FFT. Fig.5 shows the PSD of seven fault cases in the main shaft bearing.

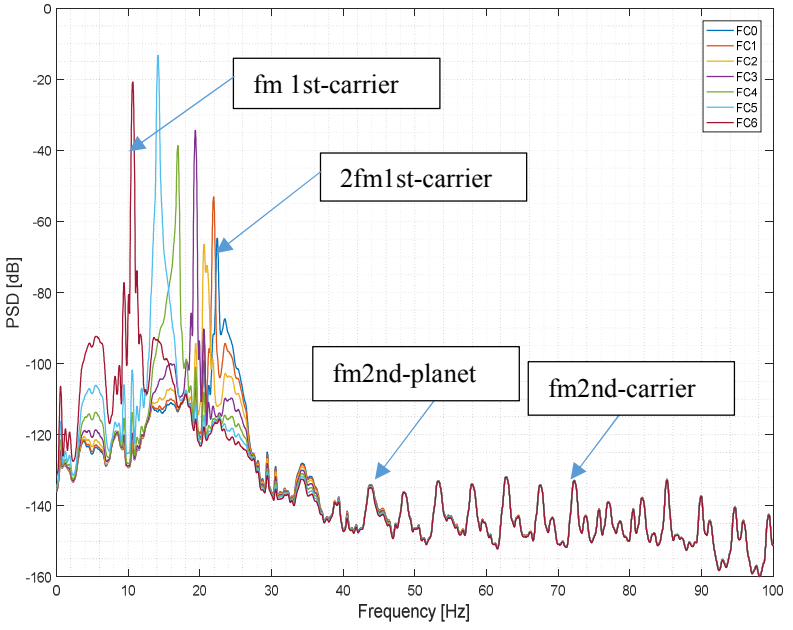

Figure 5: PSD of seven fault cases in the main shaft bearing

The INP-B main bearing is the only one carrying the axial loads induced by wind. When this bearing degrades, then the components inside the gearbox, especially in the first stage will carry more loads; this has been shown for example in [31]. Accordingly, higher vibration amplitudes at the frequencies of the first stage mesh frequency (and its harmonics) can imply that the main bearing is degrading. The dominant mesh frequency in the first stage is the carrier frequency which is 11 Hz. Due to the gear nonlinear behaviour, the sidebands in terms of integer number of mesh frequency and sum-frequency with rotational frequency are also often seen in gear system [47]. As it is shown in the Fig.5, FC1 is seen in 22 Hz which is two times of the first stage carrier mesh frequency. As the fault severity increases the frequency is shifted from two times of the mesh frequency to 11 Hz which is the mesh frequency itself. It is interesting to observe that this fault is not seen in mesh frequencies of higher stages. Therefore, depending on the fault severity of the main bearing, the fault can be detected in the mesh frequency of the first stage. In the other words, if an abnormal behaviour is observed in frequency domain anywhere between first stage mesh frequency and 2 times mesh frequency, this can be a sign of possible damage in the main bearing and/or in the first stage. If characteristic frequencies of the main bearing are known – such as ball pass frequency, ball spin frequency, etc– then it can easily be recognized whether the jump in the amplitude at the first stage mesh frequency is due to the damage in the first stage or from the main bearing.

Since IMS-B bearing is located inside the gearbox, it is not possible to instrument it directly. Using a high fidelity model is a promising approach to model nominal mode responses for fault detection of this bearing. In this respect, the angular velocity error function as introduced by Nejad et. al [26] was used. The advantage of this method is its simplicity and yet accuracy for detection prior to a catastrophic failure. Angular velocity error function, measured from output shaft and stage 2 output is served as residual using the Hilbert spectral analysis. Detection of the fault in IMS-B bearing using the same residual but with another method was investigated in [40].

Direct Fourier transform was not capable to extract useful information about the fault embedded in the angular velocity error function. A closer look at the residual Fig.6 reveals almost a narrowband relatively high frequency carrier signal and low frequency information which is embedded in the amplitude. Consequently, envelope analysis is an attractive technique. The Hilbert transform is used to obtain the envelope of the residual Fig.6. The result in Fig.7 shows that this fault is possible to be detected in mesh frequency of the planet gear in the second stage.

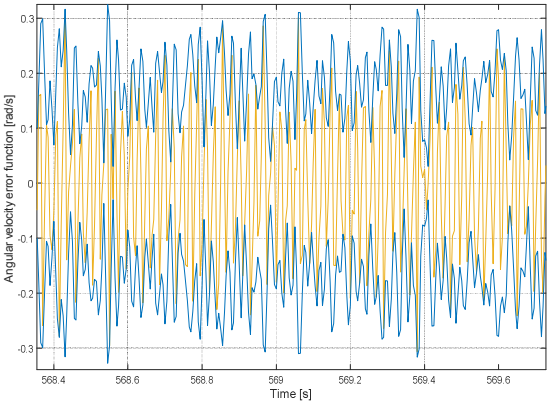

Figure 6: The angular velocity error function (yellow) and its envelope (blue)

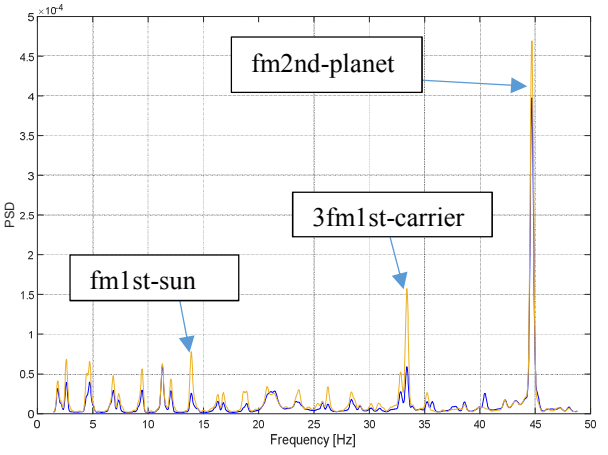

Figure 7: Envelope spectrum of the angular velocity error function.

It is expected that the damage in this bearing affects the dynamic behaviour of the planetary system in the second stage, the damage in the IMS-B bearing has increased the vibration amplitude at the planet mesh frequency. However, it should be noted that the damage at the planet or planet bearing itself can show similar results. Similar to the main bearing, if the IMS-B bearing characteristic frequencies are known, the source of the damage can be easily identified. Designing proper bandpass filters, with center frequencies set to the resonance frequencies shown above is straight

forward [40]. Then, decision is made based on the energy in the frequency bin of the filter. In cases where the resonance frequency depends on operational conditions, the center frequency of the bandpass filter may change, and probably a number of filters may be computed in advance.

5. Conclusion

In this study, fault (wear) detection in the main shaft bearing and IMS-B bearing of a 5-MW drivetrain were investigated using a high-fidelity gearbox model. Global structural analysis was first conducted using the SIMO-RIFLEX-AeroDyn software. The forces and moments on the main shaft were then applied to a high-fidelity gearbox model of a 5-MW spar-type wind turbine. Residual in order to detect wear in the main shaft bearing was obtained using relative axial acceleration of the main shaft and nacelle. It was seen that by increasing the wear severity in the main shaft bearing the resonance frequency of the relative axial acceleration moved toward the first stage carrier frequency of the bearing, giving an indication for health monitoring of this bearing for real application using global response. However, power spectral density (PSD) could only differentiate the wear greater than FC4 (50% change in the stiffness) in the main shaft bearing. Angular velocity error function served as the residual to detect the fault in IMS-B bearing, the most vulnerable bearing inside the gearbox. It was shown that the Hilbert spectral analysis could detect this fault properly.

Acknowledgements

This work has been carried out at the Center for Autonomous Marine Operations and Systems (AMOS) and the Center for Ships and Ocean Structures (CeSOS). The Norwegian Research Council is acknowledged as the main sponsor of AMOS and CeSOS. This work was supported by the Research Council of Norway through the Centers of Excellence funding scheme, project number 223254-AMOS.

References

[1] J. Ribrant, “Reliability performance and maintenance—a survey of failures in wind power systems,” *Unpublished doctoral dissertation, XR-EE-EEK*, 2006.

[2] C. A. Walford, *Wind turbine reliability: understanding and minimizing wind turbine operation and maintenance costs*: United States. Department of Energy, 2006.

[3] P. Tchakoua, R. Wamkeue, M. Ouhrouche, F. Slaoui-Hasnaoui, T. A. Tameghe, and G. Ekemb, “Wind turbine condition monitoring: State-of-the-art review, new trends, and future challenges,” *Energies,* vol. 7, no. 4, pp. 2595-2630, 2014.

[4] H. Arabian-Hoseynabadi, H. Oraee, and P. Tavner, “Failure modes and effects analysis (FMEA) for wind turbines,” *International Journal of Electrical Power & Energy Systems,* vol. 32, no. 7, pp. 817-824, 2010.

[5] Z. Jiang, M. Karimirad, and T. Moan, “Dynamic response analysis of wind turbines under blade pitch system fault, grid loss, and shutdown events,” *Wind Energy,* vol. 17, no. 9, pp. 1385-1409, 2014.

[6] E. E. Bachynski, M. Etemaddar, M. I. Kvittem, C. Luan, and T. Moan, “Dynamic analysis of floating wind turbines during pitch actuator fault, grid loss, and shutdown,” *Energy Procedia,* vol. 35, pp. 210-222, 2013.

[7] S. Faulstich, B. Hahn, and P. J. Tavner, “Wind turbine downtime and its importance for offshore deployment,” *Wind Energy,* vol. 14, no. 3, pp. 327-337, 2011.

[8] Y. Feng, Y. Qiu, C. J. Crabtree, H. Long, and P. J. Tavner, “Monitoring wind turbine gearboxes,” *Wind Energy,* vol. 16, no. 5, pp. 728-740, 2013.

[9] I. Hwang, S. Kim, Y. Kim, and C. E. Seah, “A survey of fault detection, isolation, and reconfiguration methods,” *IEEE Transactions on Control Systems Technology,* vol. 18, no. 3, pp. 636-653, 2010.

[10] M. S. Kan, A. C. Tan, and J. Mathew, “A review on prognostic techniques for non-stationary and non-linear rotating systems,” *Mechanical Systems and Signal Processing,* vol. 62, pp. 1-20, 2015.

[11] N. Perišić, P. H. Kirkegaard, and B. J. Pedersen, “Cost-effective shaft torque observer for condition monitoring of wind turbines,” *Wind Energy,* vol. 18, no. 1, pp. 1-19, 2015.

[12] S. Cho, Z. Gao, and T. Moan, “Model-based fault detection of blade pitch system in floating wind turbines,” *Journal of Physics: Conference Series,* vol. 753, no. 9, pp. 092012, 2016.

[13] S. Ilbeigi, and D. Chelidze, "Reduced order models for systems with disparate spatial and temporal scales," *Rotating Machinery, Hybrid Test Methods, Vibro-Acoustics & Laser Vibrometry, Volume 8*, pp. 447-455: Springer, 2016.

[14] E. Smilden, J.-T. H. Horn, A. J. Sørensen, and J. Amdahl, "Reduced Order Model for Control Applications in Offshore Wind Turbines," *IFAC-PapersOnLine,* vol. 49, no. 23, pp. 386-393, 2016.
[15] C. K. Tan, P. Irving, and D. Mba, "A comparative experimental study on the diagnostic and prognostic capabilities of acoustics emission, vibration and spectrometric oil analysis for spur gears," *Mechanical Systems and Signal Processing,* vol. 21, no. 1, pp. 208-233, 2007.
[16] S. Sheng, "Monitoring of Wind Turbine Gearbox Condition through Oil and Wear Debris Analysis: A Full-Scale Testing Perspective," *Tribology Transactions,* vol. 59, no. 1, pp. 149-162, 2016.
[17] M. Drewry, and G. Georgiou, "A review of NDT techniques for wind turbines," *Insight-Non-Destructive Testing and Condition Monitoring,* vol. 49, no. 3, pp. 137-141, 2007.
[18] R. Raišutis, E. Jasiūnienė, R. Šliteris, and A. Vladišauskas, "The review of non-destructive testing techniques suitable for inspection of the wind turbine blades," *Ultragarsas (ultrasound),* vol. 63, no. 1, pp. 26-30, 2008.
[19] F. Spinato, P. Tavner, G. Van Bussel, and E. Koutoulakos, "Reliability of wind turbine subassemblies," *IET Renewable Power Generation,* vol. 3, no. 4, pp. 387-401, 2009.
[20] W. Musial, S. Butterfield, and B. McNiff, "Improving wind turbine gearbox reliability," in European Wind Energy Conference, Milan, Italy, 2007, pp. 7-10.
[21] M. Ghane, A. R. Nejad, M. Blanke, Z. Gao, and T. Moan, "Statistical fault diagnosis of wind turbine drivetrain applied to a 5MW floating wind turbine," *Journal of Physics: Conference Series,* vol. 753, no. 5, pp. 052017, 2016.
[22] J. B. Ali, L. Saidi, A. Mouelhi, B. Chebel-Morello, and F. Fnaiech, "Linear feature selection and classification using PNN and SFAM neural networks for a nearly online diagnosis of bearing naturally progressing degradations," *Engineering Applications of Artificial Intelligence,* vol. 42, pp. 67-81, 2015.
[23] C. P. Mbo'o, and K. Hameyer, "Fault diagnosis of bearing damage by means of the linear discriminant analysis of stator current features from the frequency selection," *IEEE Transactions on Industry Applications,* vol. 52, no. 5, pp. 3861-3868, 2016.
[24] "ISO 15243 Rolling bearings -- Damage and failures -- Terms, characteristics and causes," 2004.
[25] M. I. Friswell, and J. E. Penny, "Crack modeling for structural health monitoring," *Structural Health Monitoring,* vol. 1, no. 2, pp. 139-148, 2002.
[26] A. R. Nejad, P. F. Odgaard, Z. Gao, and T. Moan, "A prognostic method for fault detection in wind turbine drivetrains," *Engineering Failure Analysis,* vol. 42, pp. 324-336, 2014.
[27] J. Qiu, B. B. Seth, S. Y. Liang, and C. Zhang, "Damage mechanics approach for bearing lifetime prognostics," *Mechanical systems and signal processing,* vol. 16, no. 5, pp. 817-829, 2002.
[28] A. R. Nejad, Y. Guo, Z. Gao, and T. Moan, "Development of a 5 MW reference gearbox for offshore wind turbines," *Wind Energy,* vol. 19, pp. 1089-1106, 2015.
[29] J. M. Jonkman, S. Butterfield, W. Musial, and G. Scott, "Definition of a 5-MW reference wind turbine for offshore system development," National Renewable Energy Laboratory Golden, CO, USA, 2009.
[30] J. M. Jonkman, *Definition of the Floating System for Phase IV of OC3*: Citeseer, 2010.
[31] A. R. Nejad, E. E. Bachynski, M. I. Kvittem, C. Luan, Z. Gao, and T. Moan, "Stochastic dynamic load effect and fatigue damage analysis of drivetrains in land-based and TLP, spar and semi-submersible floating wind turbines," *Marine Structures,* vol. 42, pp. 137-153, 2015.
[32] H. Ormberg, and E. E. Bachynski, "Global analysis of floating wind turbines: Code development, model sensitivity and benchmark study," in The Twenty-second International Offshore and Polar Engineering Conference, 2012.
[33] I. E. Commission, "IEC 61400-1: Wind turbines part 1: Design requirements," *International Electrotechnical Commission*, 2005.
[34] L. Li, Z. Gao, and T. Moan, "Joint distribution of environmental condition at five european offshore sites for design of combined wind and wave energy devices," *Journal of Offshore Mechanics and Arctic Engineering,* vol. 137, no. 3, pp. 031901, 2015.
[35] M. I. Kvittem, and T. Moan, "Time domain analysis procedures for fatigue assessment of a semi-submersible wind turbine," *Marine Structures,* vol. 40, pp. 38-59, 2015.
[36] Y. Xing, M. Karimirad, and T. Moan, "Modelling and analysis of floating spar-type wind turbine drivetrain," *Wind Energy,* vol. 17, no. 4, pp. 565-587, 2014.
[37] A. R. Nejad, Z. Gao, and T. Moan, "On long-term fatigue damage and reliability analysis of gears under wind loads in offshore wind turbine drivetrains," *International Journal of Fatigue,* vol. 61, pp. 116-128, 2014.

[38] A. R. Nejad, Z. Jiang, Z. Gao, and T. Moan, “Drivetrain load effects in a 5-MW bottom-fixed wind turbine under blade-pitch fault condition and emergency shutdown,” in Journal of Physics: Conference Series, 2016, pp. 112011.
[39] I. O. f. Standardization, "ISO 20816-1:2016," *Mechanical vibration - Measurement and evaluation of machine vibration - Part 1: General guidelines*, 2016.
[40] P. F. Odgaard, and A. R. Nejad, “Frequency based wind turbine gearbox fault detection applied to a 750 kW wind turbine,” in 2014 IEEE Conference on Control Applications (CCA), 2014, pp. 1383-1388.
[41] A. Carcaterra, and A. Sestieri, “Complex envelope displacement analysis: a quasi-static approach to vibrations,” *Journal of Sound and Vibration,* vol. 201, no. 2, pp. 205-233, 1997.
[42] J. J. Zakrajsek, R. F. Handschuh, D. G. Lewicki, and H. J. Decker, *Detecting Gear Tooth Fracture in a High Contact Ratio Face Gear Mesh*, DTIC Document, 1995.
[43] W. T. Peter, Y. Peng, and R. Yam, “Wavelet analysis and envelope detection for rolling element bearing fault diagnosis—their effectiveness and flexibilities,” *Journal of vibration and acoustics,* vol. 123, no. 3, pp. 303-310, 2001.
[44] X. Fan, and M. J. Zuo, “Gearbox fault detection using Hilbert and wavelet packet transform,” *Mechanical systems and Signal processing,* vol. 20, no. 4, pp. 966-982, 2006.
[45] B. Liu, S. Riemenschneider, and Y. Xu, “Gearbox fault diagnosis using empirical mode decomposition and Hilbert spectrum,” *Mechanical Systems and Signal Processing,* vol. 20, no. 3, pp. 718-734, 2006.
[46] R. B. Randall, *Vibration-based condition monitoring: industrial, aerospace and automotive applications*: John Wiley & Sons, 2011.
[47] A. R. Nejad, Y. Xing, and T. Moan, “Gear train internal dynamics in large offshore wind turbines,” in ASME 2012 11th Biennial Conference on Engineering Systems Design and Analysis, 2012, pp. 823-831.